

HEAT TRANSFER, THERMAL STRESS ANALYSIS AND THE DYNAMIC BEHAVIOUR OF HIGH POWER RF STRUCTURES

J. McKeown and J.-P. Labrie

Atomic Energy of Canada Limited, Research Company  
Chalk River Nuclear Laboratories  
Chalk River, Ontario, Canada K0J 1J0

Summary

A general purpose finite element computer code called MARC is used to calculate the temperature distribution and dimensional changes in linear accelerator rf structures. Both steady state and transient behaviour are examined with the computer model. Combining results from MARC with the cavity evaluation computer code SUPERFISH, the static and dynamic behaviour of a structure under power is investigated. Structure cooling is studied to minimize loss in shunt impedance and frequency shifts during high power operation. Results are compared with an experimental test carried out on a cw 805 MHz on-axis coupled structure at an energy gradient of 1.8 MeV/m. The model has also been used to compare the performance of on-axis and coaxial structures and has guided the mechanical design of structures suitable for average gradients in excess of 2.0 MeV/m at 2.45 GHz.

Introduction

Computer codes such as SUPERFISH<sup>1</sup>, PRUD<sup>2</sup> and BCI<sup>3</sup> continue to make great contributions in optimizing the efficiency of rf structures. However, operational behaviour such as loss of shunt impedance, field redistribution through thermal detuning and transient beam loading must be studied experimentally. A more comprehensive model with a new generation of computer codes is needed to take account of these effects.

In this paper an extension of the analysis of rf structures is made that includes not only the electromagnetic properties but also heat transfer and thermal stress. The PETRA cavity<sup>4</sup> is used as an example and measurements of thermal distributions in the Mainz cavity<sup>5</sup> and in the Electron Test Accelerator cavity<sup>6</sup> are compared with calculations using mesh representations of these structures. Different cooling schemes are investigated and the dimensional stability under thermal stress of the on-axis structure and the coaxial structure<sup>7</sup> is compared. Finally, transient thermal behaviour calculated by the computer model is compared with experiment.

Application of Models to Cavity Design

A cavity shape is usually optimized by using a finite difference mesh code like SUPERFISH to calculate the rf efficiency for any given geometry. The surface power distribution calculated by SUPERFISH has been used in the finite element computer code MARC<sup>8</sup> to calculate the temperature distributions in cavities under different cooling conditions. Steady state temperature distributions in rf cavities have been obtained previously with the computer code DOT<sup>9</sup> and a new version of SUPERFISH<sup>10</sup>. MARC however provides elastic, large displacement buckling stress and heat transfer analysis capabilities. It adds the possibility of predicting dimensional changes in rf cavities both under steady state and transient conditions. Using the displacements from MARC as input to SUPERFISH the frequency shifts resulting from thermal expansion of rf structures for given power levels and cooling conditions are calculable.

Heat Transfer and Thermal Stress Analysis

A mesh generator is used in MARC to divide the cavity geometry into a finite number of elements having their boundaries defined by a series of nodes. Physical properties for each mesh element such as thermal conductivity, specific heat and thermal expansion coefficients are given as input.

The first step in a thermal stress analysis problem is to establish the temperature distribution for a given time interval. Figure 1(a) shows the steady state temperature distribution for the PETRA cavity (500 MHz) at 1.0 MeV/m when only circumferential cooling is used. Figure 1(b) shows a similar distribution for the Mainz cavity (2.45 GHz) at the same gradient with the same cooling. For the latter cavity, the temperature along the web has been measured<sup>11</sup>. These experiments found a nose cone temperature of 16.5°C above the outer surface at a power level of 13 kW/m. Our calculations at a power level of 15 kW/m estimate the incremental nose cone temperature to be 12°C. The discrepancy may be accounted for by the coupling slots which cannot be modeled with axially symmetric mesh generators.

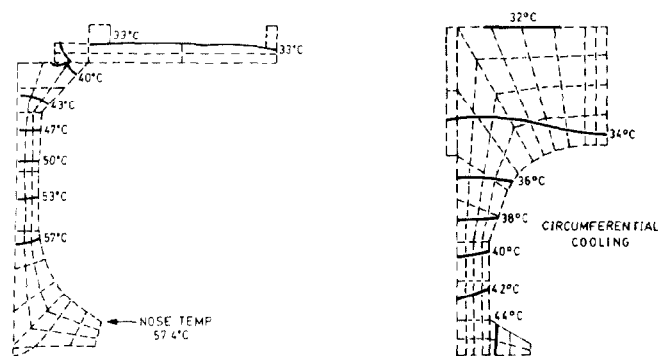


Fig. 1 (a) Temperature distribution of PETRA cavity. (b) Temperature distribution of Mainz cavity.

Figure 2 shows the effect of using radial cooling for the PETRA and the Mainz cavities at an energy gradient of 1.0 MeV/m. Radial cooling reduces the loss in shunt impedance from the increase in resistivity due to higher temperatures. Similar calculations were done for an on-axis coupled structure undergoing tests at Chalk River. With both types of cooling employed the calculations were compared with the experimental measurements taken with an 805 MHz structure operating at 105 kW/m (1.8 MeV/m). The calculated average surface incremental temperature of 5.5°C can be compared with the measured distribution in Fig. 3. Agreement is good except in areas near stainless steel flanges or other localized hot spots.

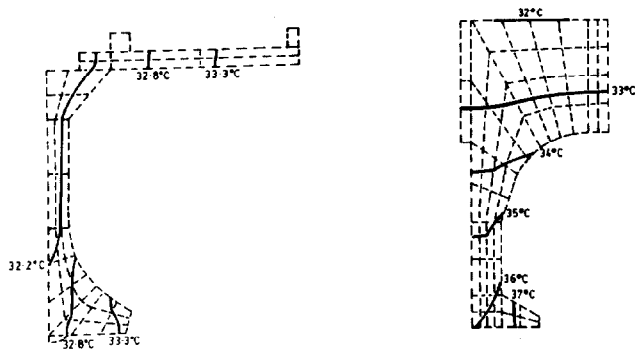


Fig. 2 (a) Temperature distribution of PETRA cavity with radial coolant flow of 1.67 L/s.  
 (b) Temperature distribution of Mainz cavity with radial coolant flow of 0.6 L/s.

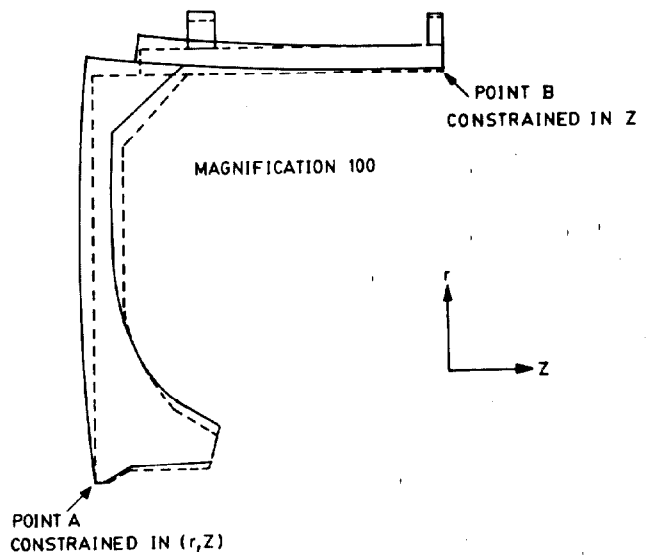


Fig. 4 Deformation of end cell of PETRA with gradient of 1 MeV/m and circumferential cooling only.

A biperiodic system is chosen for high average power use because of its longitudinal field cavity-to-cavity stability. An on-axis system allows direct transfer of the detuning of the accelerating cavity to the coupling cavity through the common segment wall. As the coupling cavity is about an order of magnitude more sensitive to dimensional changes, calculations were carried out with the on-axis structure and compared with calculations on the coaxial structure where the nose cones of adjoining accelerating cavities form an integral unit. For both structures, identical circumferential cooling is used and Fig. 5 shows the dimensional changes at 1.0 MeV/m amplified by a factor of 1000. The nose cone area of both structures penetrates into the accelerating cavity volume but it is to be expected that its effect would be much less than the distortion of the coupling cavity.

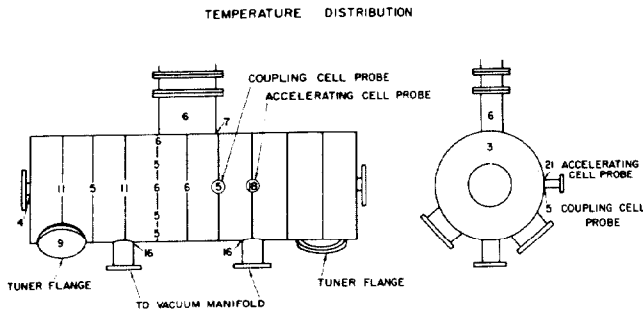


Fig. 3 Measured surface temperatures for on-axis structure at 805 MHz with gradient 1.8 MeV/m. The numbers refer to temperatures in °C above the inlet water temperature. The values away from the accelerating cell probes are indicative of the copper temperature calculated for the idealized symmetrical model.

SUPERFISH is used to determine the resultant frequency shifts. Table 1 gives the thermal detuning sensitivity for the two structures mentioned above. The accelerating cell of the coaxial structure is almost twice as sensitive while both coupling cells change by equal amounts. The change in stopband, which is the defining parameter for thermal detuning, is about 70% greater in the on-axis case, however both are still within acceptable tuning tolerances.

The second step in the analysis is to use the calculated temperatures at a given time and perform a stress analysis to calculate the displacement of the nodal points. Figure 4 shows how the shape of an end cell in the PETRA cavity changes from the isothermal condition to full power operation. The expansion into regions of high electric field and away from regions of high magnetic field explains why the resonant frequency of the cavity decreases with increasing power.

Thermal Detuning

Temperature gradients exist because it is impracticable to design the cooling system to counteract fully the effect of the wall rf currents excited by the accelerating mode. Compensation of these frequency shifts by localized tuners in coupled resonator systems leads to further detuning.

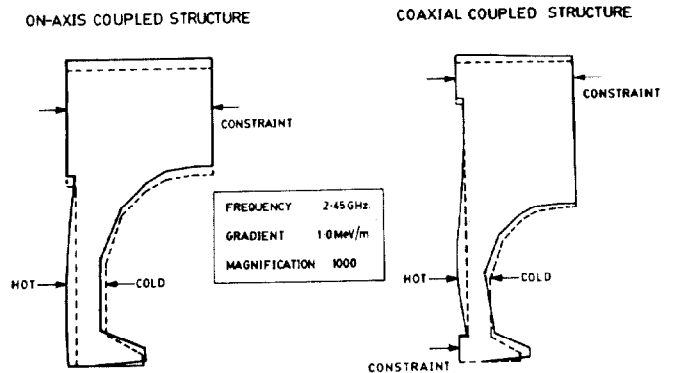


Fig. 5 Comparison of deformations of two biperiodic structures.

### Transient Behaviour

Steady state and temperature transients were measured in an 805 MHz on-axis coupled structure having both circumferential and radial cooling channels. The frequency shift with only circumferential flow is 280 kHz at 50 kW/m. This shift is reduced five-fold if radial flow is also used. This difference indicates that although calorimetric measurements show that radial cooling carries away less than 30% of the total power, it is more effective in reducing frequency shifts in high gradient structures.

The dynamic response of radial and circumferential cooling in the 805 MHz structure is shown in Fig. 6. The rapid increase in frequency of 15 kHz/s when one half of the radial counterflow circuit is turned on is duplicated when the second half is opened. This contrasts with the 0.75 kHz/s when the same experiment is carried out with the circumferential cooling. Calculations using MARC and SUPERFISH under these conditions give steady state frequency shifts about a factor of three smaller than the observed values. The Fourier transforms of the frequency shift of the two cooling schemes are not significantly different indicating that the constraining forces used in the model must be further refined.

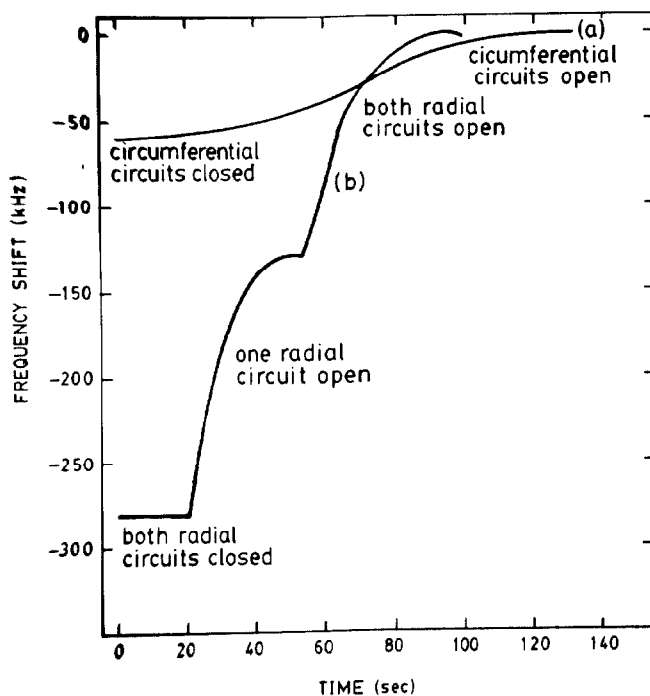


Fig. 6 (a) Frequency shifts when circumferential cooling is turned on at 50 kW dissipation in a 1 m on-axis structure operating at 805 MHz.  
(b) Frequency shifts when radial cooling is turned on at 50 kW dissipation in 1 m on-axis structure operating at 805 MHz.

Table 1 Thermal Detuning Sensitivity  
(2.45 GHz, 1 MeV/m, circumferential cooling)

	Accelerating Mode	Coupling Mode	Change in Stopband
On-axis	-0.00922%	-0.0329%	632 kHz*
Coaxial	-0.0142%	-0.0297%	371 kHz

\*The measured value <sup>11</sup> for the change in stopband in the on-axis structure is 460 kHz.

### Conclusions

The computer code MARC has been used to calculate temperature distributions in rf structures. Guidance in the mechanical design of structures for more efficient operation at high gradient is now possible. Thermal stress analysis correctly predicts the direction of frequency shifts and provides a method of testing the relative sensitivity of different structures to thermal detuning. Calculation of transient response during start-up and cooling flow changes is limited by the representation of the structure's constraints.

### Acknowledgement

The authors thankfully acknowledge the assistance of H. Hatton for initially testing our model with results published on the LEP cavity<sup>9</sup>.

1. K.H. Halbach and R.F. Holsinger, "SUPERFISH - A Computer Program for Evaluation of Rf Cavities with Cylindrical Symmetry", *Particle Accelerators* 7 (1976) 213.
2. A.G. Daikovsky, Yu. I. Portugalov and A.D. Ryabov, "PRUD - Code for Calculation of Non-Symmetric Modes in Axial Symmetric Cavity", *Particle Accelerators* 12 (1982) 59.
3. T. Weiland, "On the Computation of Electromagnetic Fields Excited by Relativistic Bunches of Charged Particles in Accelerating Structures", CERN report, CERN/ISR-TH/80-07 (January 1980).
4. H. Gerke et al., "Das PETRA-Cavity", *Internes Bericht DESY PET-77/08* (1977).
5. H. Euteneuer, "Design, Performance and Blow-up Properties of the MAMI-Structure", *Proc. of the Conf. on Future Possibilities for Electron Accelerators*, University of Virginia, January 1979, P-1.
6. J. McKeown et al., "High Power, On-axis Coupled Linac Structure", *Proc. of the 1981 Linear Accelerator Conference*, Santa Fe, NM, LA-9234-C (1982) 332.
7. J.-P. Labrie and J. McKeown, "The Coaxial Coupled Linac Structure", *Nucl. Inst. & Meth.* 193 (1982) 437-444.
8. MARC, Marc Analysis Research Corporation, 260 Sheridan Ave., Palo Alto, CA 94306, USA.
9. H. Henke and I. Wilson, "Thermal Analysis and Loss in Shunt Impedance of the LEP Accelerating Cell", CERN/ISR-RF-GE/81-25, LEP Note 309.
10. S.O. Schriber and R.F. Holsinger, "Additions and Improvements to the Rf Cavity Code SUPERFISH", this conference.
11. H. Euteneuer, private communication.